

## JOINT IMAGING OF VELOCITY AND FLAME FRONT MOVEMENT IN A TURBULENT PREMIXED FLAME

P. A. M. Kalt, S. H. Stårner and R. W. Bilger

Department of Mechanical and Mechatronic Engineering  
University of Sydney  
Sydney, New South Wales  
Australia

### ABSTRACT

Particle image velocimetry has been used to determine the velocity vector field in a turbulent premixed Vee-flame, using a double-pulsed Nd:YAG laser and a CCD camera, the velocity information and the location of the flame front in the plane of the laser sheet were simultaneously resolved. A second CCD camera and a flashlamp pumped dye laser, coincident with the Nd:YAG laser sheet, were used to determine the location of the flame front after a short interval, enabling calculation of the flame speed,  $S_u$ , as the difference of the apparent flame velocity and the flow velocity. A positive correlation between  $S_u$  and the curvature of the flame front,  $h$ , is observed. Average values for  $S_u$  are somewhat above predictions for an unstrained laminar flame.

### INTRODUCTION

Combustion in spark ignition engines and many gas explosions is governed by the rate of propagation of a thin front that lies between the unburnt mixture and burnt gas. The fluid is turbulent and the front propagates relative to this turbulent velocity field. Because of its economic importance the turbulent premixed flame has been subject to intensive study for many decades.

Theories of turbulent premixed flame propagation (Bray 1990, Bradley 1993) are not, however, in a satisfactory state and give inadequate correlation of experimental data on turbulent flame speed. The problem is quite complex and progress has been limited by the difficulties of making accurate detailed measurements of the flame structure. Most theories assume that locally the flame is very thin and behaves as a strained and curved laminar flame (Peters 1988). Recent measurements by Rayleigh scattering and laser induced fluorescence (O'Young and Bilger 1995, Dinkelacker et al 1993) indicate that the temperature and species concentrations are not consistent with this "laminar flamelet" assumption. Our work here is aimed at developing techniques to find out whether the laminar flamelet assumption is valid for the kinematics of the flame front motion.

Particle Image Velocimetry (PIV) has been developed (Adrian 1991) to give high quality measurements of the velocity field of the flow, or rather components of it in

the image plane. The technique has been applied in combustion (Echekki and Mungal 1991) but in turbulent flow (Lecordier et al 1994) there are considerable problems with the large dynamic range needed. Here we extend the technique to also measure the propagation speed of the front itself so that the speed of the front relative to the unburnt mixture,  $S_u$ , (referred to as the flame speed below) can be determined. This is done by using a second laser and camera to measure the flame front position at a time interval much larger than the double pulse used to measure the velocity field.

Dynamic range problems are avoided by working in a Vee-flame with moderate turbulence level. Analysis is made of the relationship between the local flame speed and the curvature of the flame front.

### EXPERIMENTAL SET-UP

The propane air mixture (equivalence ratio  $\phi=1.2$ ) issues from a 36mm diameter nozzle at 4.7m/s into a laminar co-flowing stream and is densely seeded with micron sized particles of  $\text{TiO}_2$  generated by reacting  $\text{TiCl}_4$  with  $\text{H}_2\text{O}$  vapour in the fuel/air mixture. This method is found to yield superior spatial uniformity and a narrower seed size distribution than by introducing solid particles aerodynamically. A photodiode monitors the seeding density in the flame to ensure that a steady seeding level is maintained.

Turbulence in the fuel/air stream is generated by a plate with 6mm holes at 6.35mm spacing, inserted 80mm upstream of the nozzle exit. The flame is stabilised on a wire of thickness 1.6mm located 34mm above the burner exit and 8mm off axis. The rms turbulence,  $u'$ , is  $0.49\text{ms}^{-1}$  at the measurement location, 35-57mm above the nozzle exit.

The location of the image relative to the wire has been chosen so that the wake effects from the flow around the wire were absent in the region of the flame being interrogated. The bore of the burner is large so that the unburnt region near the flame contains only seeded fuel/air mixture, and no unseeded air is mixed in from the filtered air coflow. This is verified by imaging in the unignited stream: the whole image has a uniform seeding distribution.



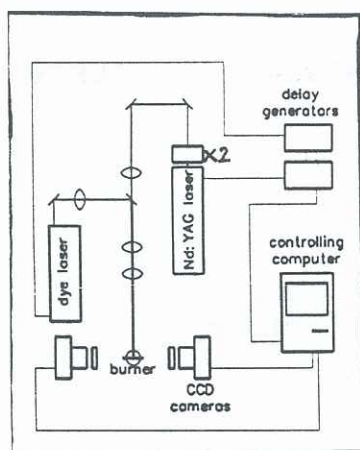


Figure 1: Schematic experimental set-up

### Imaging System

The beams from both the flashlamp pumped dye laser and the Nd:YAG laser are collimated to form coincident sheets approximately 0.7mm thick and 22mm high (Fig. 1). The beam from the Nd:YAG laser is passed through a doubling crystal to emerge at 532nm wavelength. The dye laser is tuned to a wavelength of 550nm. Both CCD cameras use interference filters to pass only the Mie scattering of the required wavelength, since the slow shutter speeds on the CCD cameras result in the shutters on both cameras remaining open for all three laser pulses. The images from the CCD cameras are 384 pixels high and 576 pixels across. Each pixel corresponds to 27 $\mu$ m in the flame.

Both PIV pulses from the double-pulsed Nd:YAG laser (pulse separation = 40  $\mu$ s) were recorded on one camera (Fig. 2). This image is then used to determine the velocity vector field using an autocorrelation technique. The PIV image is high pass filtered to remove background, and passed through a function that takes the natural logarithm of the intensity to reduce the intensity difference between particle pairs. This is advantageous for the subsequent Fourier transform analysis of the 2.9mm<sup>2</sup> (64 pixel by 64 pixel) sub-domains that define the spatial resolution. The subdomains overlap: the increment is 16 pixels so that there is substantial overlapping between adjacent vectors. Figure 3 shows a typical PIV vector field, which contains a large number of vectors that change smoothly over the image, suitable for translating the Nd:YAG image. There is adequate seeding density also in the burnt fluid for velocity determination, although this is not clear in Fig. 2.

### Flame Front Processing

Information about the flame front location is obtained from the PIV image (Fig. 2) and the image from the second CCD camera (Fig. 4), using the Mie scattering from the dye laser, 204 $\mu$ s after the first Nd:YAG laser pulse.

Very high seeding density (up to 1000/mm<sup>3</sup>) is required to resolve the flame front. Tests with varying seed levels reveal that although many particles may overlap in each pixel, this does not corrupt the PIV data.

The location of the flame front is determined by the change in number density of the TiO<sub>2</sub> particles as they pass into the burnt zone. A reduction in the Mie

scattering cross section of TiO<sub>2</sub> due to the temperature increase across the flame front further enhances the contrast between the burnt and unburnt regions of the image. The resulting intensity ratio is approximately 15.

The flame front is arbitrarily defined as the location of the maximum intensity gradient in the smoothed images. As this procedure is used in both images, any systematic bias is expected to cancel.

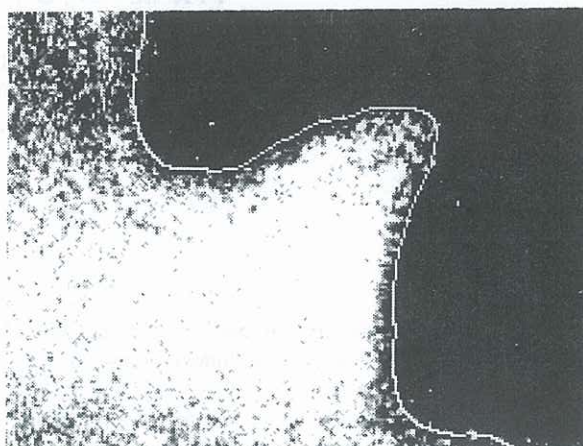


Figure 2: Nd:YAG laser image with enhanced flame front

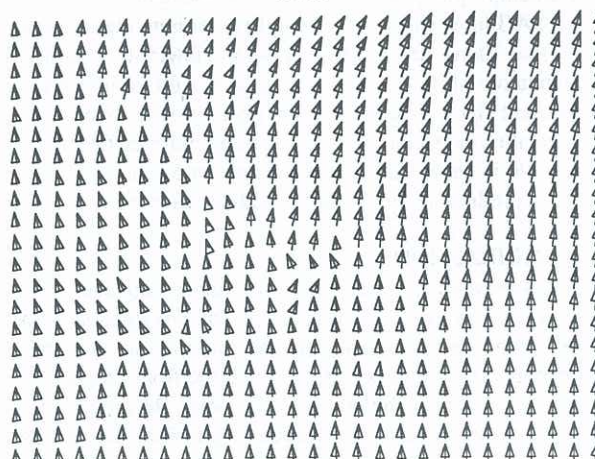


Figure 3: Velocity vector field from Nd:YAG image

### Image Translation

The PIV image contains the particle images corresponding to the two Nd:YAG pulses ( $t = t_0$  and  $t = t_0 + 40\mu$ s). The flame front determined from this image is assumed to be equivalent to the flame front location at a time mid-between the two pulses. This is verified by taking dye laser images at  $t = t_0 + 20\mu$ s, and comparing the flame front images obtained. It is found that the error involved in this procedure is less than 0.05mm (less than 2 pixels).

The flame front obtained from the PIV image is translated by the product of the local (unburnt) velocity vector and  $\delta t$  ( $\delta t$  is the time between the laser pulses, and the first pulse time is taken as the average for the two PIV shots). Superposition of the translated (first) image on the second image (Fig. 5) yields the flame front



movement in time  $\delta t$ , so that the local flame speed,  $S_u$ , can be obtained.

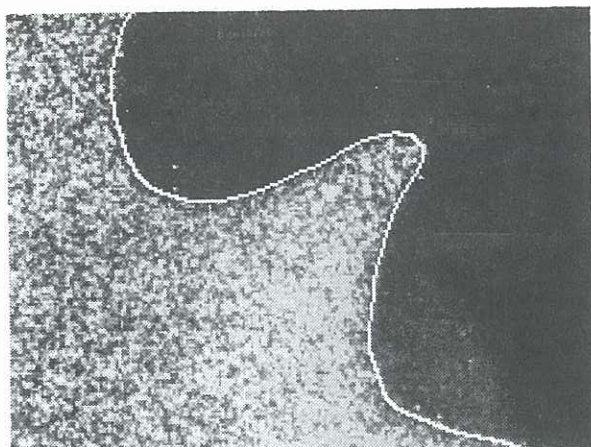


Figure 4: Dye laser image with enhanced flame front

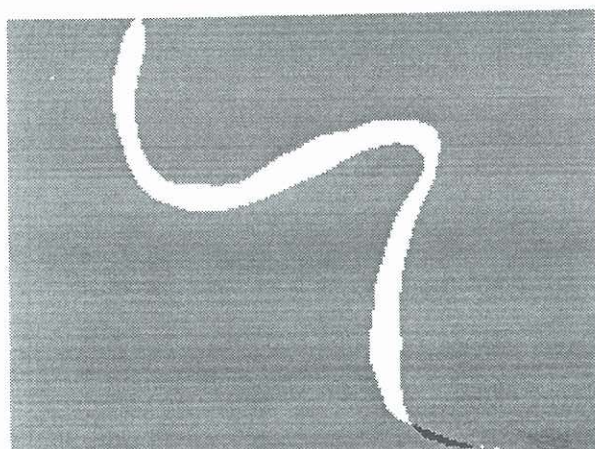


Figure 5: Image showing superposed flame fronts from translated Nd:YAG image and dye laser image.

Shifting the flame front of the first image by the derived vector field can introduce errors to the flame front position. The technique requires a very well resolved velocity field as  $S_u$  is in effect derived as the difference between the fluid velocity and the apparent flame velocity. Both these quantities are typically larger than  $S_u$ , so noise and bias effects are magnified. Whilst random noise may cancel in averaging, any bias in the technique must be identified and corrected, as discussed below.

## RESULTS AND DISCUSSION

A survey of many images of rich and lean flames indicates that large, often cusp-shaped excursions of unburnt fuel/air mixture move into the burnt zone more commonly for rich flames than for lean flames. (The opposite, i.e., cusps of burnt fluid pointing into the fresh mixture, is not apparent.)

The PIV vector field represents the flow velocity,  $\underline{U}$ , in the image plane (Fig. 3). It is seen that the spatial

variation in  $\underline{U}$  is not large, i.e. the dynamic range required of the PIV system is modest, and the flow is everywhere far from reversal. A marked increase in velocity is observed across the flame front; there is also some change of direction near the reaction zone, as expected.

In Fig. 5, the width of the band between the two flame fronts is a linear representation of the local flame speed,  $S_u$ . Such an image would show the true value of  $S_u$  only when the flame front is normal to the image plane. The white area in Fig. 5 represents positive  $S_u$ ; the black area indicates negative  $S_u$ . This apparent negative  $S_u$  is thought to be caused by oblique alignment of the flame front relative to the image plane. This effect is best analysed by considering displacement due to turbulent motion and laminar flame propagation separately: The effect of obliquely aligned flame propagation alone is to increase the measured flame speed,  $S_{u(meas)}$ :  $S_{u(meas)} = S_{u(true)} / \sin \alpha$ , where  $\alpha$  is the angle between the flame front and the laser sheet. A first order correction for this effect has been made here by making the assumption that in this relatively low-turbulence flame, the flame front thickness,  $w$ , does not vary greatly. With this assumption, the measured width,  $w_m$ , (using the dye laser images only) is used to correct  $S_u$ :  $S_{u(corr)} = S_{u(meas)} w_{min}/w$ , where  $w_{min}$  is the measured minimum width for the data set, taken to represent orthogonal alignment ( $\alpha = \pi/2$ ). This correction reduces the measured mean flame speed,  $\langle S_u \rangle$ , (averaged over 10 images) from  $1.20 \text{ ms}^{-1}$  to  $0.61 \text{ ms}^{-1}$ , and the rms,  $S_u'$ , from  $0.48 \text{ ms}^{-1}$  to  $0.25 \text{ ms}^{-1}$ . However, turbulent motion has a different effect on measured  $S_u$ : Where an obliquely aligned flame front is convected by turbulence in the  $z$ -direction (i.e. orthogonally to the image plane),  $S_{u(meas)}$  is either increased or decreased, depending on the direction of motion relative to the unburnt fluid. Large transverse motion coupled with very oblique alignment is the main cause of the occurrence of negative values of  $S_u$  as well as some unrealistically large positive values. Correction for this effect would require some form of 3D measurements and would be essential where  $S_u'$  is sought. However, we can use a symmetry condition, namely that the velocity component  $u_z$  should be symmetrically distributed around zero, to argue that the effect on the mean,  $\langle S_u \rangle$ , should be zero.

It is thus found that measured  $\langle S_u \rangle$  in this turbulent flame is somewhat larger than the  $0.5 \text{ ms}^{-1}$  value expected in a similar laminar flame.

Figure 6 shows the curvature  $h$  of the flame front in Fig. 4 (where  $h$  is defined as the inverse of the radius of curvature, and positive curvature is defined as that in an expanding spherical flame ball). Here, the colour of the band, rather than its width, indicates the value of  $h$ . If the assumption is made that  $u_z$  and  $h$  are statistically independent, the out-of-plane component of  $R_{Su,h}$  averages to zero so that  $R_{Su,h}$  should not be biased even though only the in-plane components are recorded here.

Computed values of  $R_{Su,h}$  for individual images of the rich flame (equivalence ratio 1.2) vary in sign but are typically very low ( $|R_{Su,h}| < 0.15$ ), with the average for the data set an insignificant  $-0.03$ . Theory as well as experiments by others (see the review by Law, 1989) imply a negative value in a rich ( $Le < 1$ ) propane flame:



elements of the flame surface with positive curvature are expected to burn more slowly while negatively curved elements of the flame front should burn more quickly. However, this limited data set does not show a significant trend.

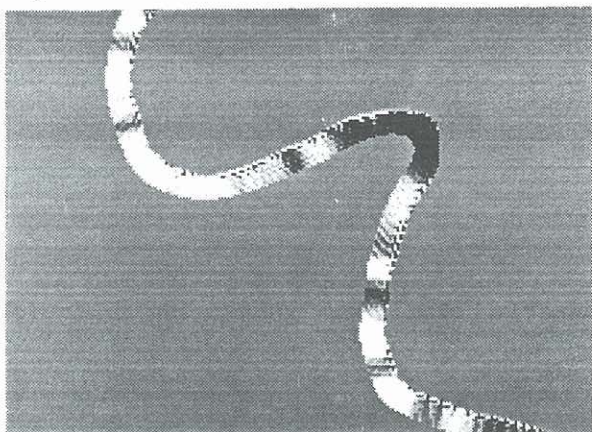


Figure. 6: Curvature image of the flame front (positive curvature light, negative curvature dark). Burnt fluid on right side.

## CONCLUSIONS

This preliminary study demonstrates the feasibility of obtaining simultaneous, quantitative data on flame front movement and velocity in a moderately turbulent flame, using a fairly simple 2D Mie scattering technique. The limited results processed to date are plausible, but it is clear that in the absence of joint measurements in the third dimension to map flame orientation, the results are distorted by oblique alignment. Only very simplified corrections can be made to account for obliqueness, and direct measurements of local flame front thickness are precluded. In view of the long-term aim to explore the validity of flamelet theory in highly turbulent flames, these are serious shortcomings. In addition, in such flames, where  $u'/S_u$  is very large, the determination of  $S_u$  as the difference between two much larger velocities will require very accurate measurements if significant findings are to emerge.

A 2D burner with forced, periodic flow is now under development to enable close scrutiny of potential bias and other errors associated with this method.

It is intended to develop this technique on a scale where flow kinematics can be resolved within the distributed reaction zone. Autocorrelation PIV techniques introduce difficulties in resolving flows with reversals, present in most turbulent flame structures of interest. Two-image cross correlation PIV may be introduced into this technique so that ultimately small scale changes inside the flames with flow reversals can be resolved. In addition, a further laser sheet and camera system will be needed to map flame orientation.

## ACKNOWLEDGMENTS

This work is supported by a grant from the Australian Research Council.

## REFERENCES

- Adrian, R. J., 1991, "Particle-imaging techniques for experimental fluid mechanics", *Annu. Rev. Fluid Mech.*, Annual Reviews Inc, pp. 261-304.
- Bradley, D., 1992, "How fast can we burn?", *Twenty-fourth Symposium (International) on Combustion*, The Combustion Institute, pp. 247-261.
- Bray, K. N. C., 1990, "Studies of the turbulent burning velocity", *Proc. R. Soc. Lond.* A431, pp. 315.
- Dinkelacker, F., Buschmann, A., Schäfer, M. and Wolfrum, J., 1993, "Spatially resolved joint measurements of OH and temperature fields in a large premixed turbulent flame", *Proc. Anglo-German Combustion Symposium*, pp. 295-298.
- Echekki, T., and Mungal, M. G., "Flame speed measurements at the tip of a slot burner: Effects of flame curvature and hydrodynamic stretch", *Twenty-third Symposium (International) on Combustion*, The Combustion Institute, pp. 455-461.
- Law, C.K., 1989, "Dynamics of stretched flames", *Twenty-second Symposium (International) on Combustion*, The Combustion Institute, pp. 1381-1402.
- Lecordier, B., Mouqualid, M. and Trinité, M., 1994, "Simultaneous 2D measurements of flame front propagation by high speed tomography and velocity field by cross correlation", *Proceedings, Seventh Nit. Sump. on Applications of Laser Techniques to Fluid Mech.*, Lisbon, pp. 15.2.1-15.2.8.
- O'Young, F. and Bilger, R. W., 1995, "Measurement of scalar dissipation in premixed flames", *Comb. Sci. Tech. (Under review)*
- Peters, N., 1988, "Laminar flamelet concepts in turbulent combustion", *Twenty-first Symposium (International) on Combustion*, The Combustion Institute, pp. 1231-1250.